Carbohydrate Polymers 106 (2014) 247–254

Contents lists available at ScienceDirect

Carbohydrate Polymers

journal homepage: www.elsevier.com/locate/carbpol

# Structural identification and sulfated modification of an antiglycation *Dendrobium huoshanense* polysaccharide

Xiao-Long Li, Jing-Jing Xiao, Xue-Qiang Zha*, Li-Hua Pan, Muhammad-Naeem Asghar, Jian-Ping Luo*

*School of Biotechnology and Food Engineering, Hefei University of Technology, No. 193, Tunxi Road, Hefei 230009, People's Republic of China*

ARTICLE INFO

*Article history:*
Received 14 January 2014
Received in revised form 7 February 2014
Accepted 8 February 2014
Available online 17 February 2014

*Keywords:*
*Dendrobium huoshanense*
Polysaccharide
Sulfation
Antiglycation

ABSTRACT

*Dendrobium huoshanense*, an important food material, has been used to make teas and soups in the folk of China for centuries. In the present study, an antiglycation polysaccharide DHPD2 with molecular weight of $8.09 \times 10^6$ Da was extracted from the protocorm-like bodies of *D. huoshanense*. The backbone of DHPD2 contained (1→5)-linked α-L-Ara*f*, (1→6)-linked α-D-Glc*p*, (1→6)-linked β-D-Glc*p*, (1→4)-linked β-D-Glc*p*, (1→3,6)-linked β-D-Gal*p* and (1→6)-linked β-D-Gal*p*, with the branches of terminal α-D-Xly*p* and β-D-Man*p*. DHPD2 was further modified using chlorosulfonic acid–pyridine method, giving two sulfated derivatives with the substitution degree of 0.475 and 0.940. The appearance of two new characteristic absorption bands at near 1250 and 822 $cm^{-1}$ in FT-IR spectra revealed the success of sulfation occurred to DHPD2. Moreover, the sulfated derivatives exhibited stronger inhibitory abilities on protein glycation than those of DHPD2. NMR analysis disclosed that the sulfation on C2 and C6 of sugar residues was beneficial to enhance this activity.



## 1. Introduction

Protein glycation is a complicated reaction process between aldehydic group in reducing sugar and amino group in proteins, resulting in the formation of advanced glycation end products (AGEs) (Wang, Zhang, & Dong, 2012). The AGEs have been confirmed to be implicated in the pathogenesis of some chronic diseases including aging, Alzheimer's disease and diabetic complications (J. Wang, Sun, Cao, & Tian, 2009). The suppression of AGE accumulation is therefore expected to be an effective treatment of these diseases. It has been reported that long-term treatment of compounds with antiglycation properties is beneficial for prevention of diabetic complications in experimental animals (Jagtap & Patil, 2010; Kumar, Reddy, Srinivas, & Reddy, 2009; Wada et al., 2002). Some AGE inhibitors including aminoguanidine, benfotiamine and pyridoxamine, have been used in clinical trials. However, these compounds were reported to have serious toxicities (Singh, Barden, Mori, & Beilin, 2001). In recent years, there is an increasing interest in screening AGE inhibitors from natural sources, due to their low toxicity.

*Dendrobium huoshanense* C.Z. Tang et S.J. Cheng, an important Orchidanceae family plant, has been used as a food material to make teas and soups in the folk of China for centuries (Huang & Zhang, 2000). According to the ancient Chinese literatures, *D. huoshanense* was recorded to improve a wide range of health problems such as yin-yang disharmony and weak eyesight (Liu & Luo, 2005). To understand these health functions, many compounds including alkaloids, free amino acids and polysaccharides have been extracted and isolated from this species in the last few years (Hsieh et al., 2008). Among these compounds, polysaccharides were reported to be the main factors responsible for the health benefits of *D. huoshanense*, exhibiting anti-tumor, anti-oxidant and immunomodulating activities (Hsieh et al., 2008). In our ongoing research for the bioactive constituents in this plant, we found that the crude polysaccharides of *D. huoshanense* (DHP) had good potential for preventing mouse diabetic cataract genesis induced by streptozotocin (Li, Deng, Pan, Huang, & Luo, 2012; Luo, Deng, & Zha, 2008). This ability was disclosed to be mainly due to their inhibitory effects on protein glycation in lens (Luo et al., 2008). However, the chemical structure of antiglycation polysaccharides in this species is still unknown.

In an effort to discover the new information of natural health products, the present study was undertaken to investigate the structural features of *D. huoshanense* polysaccharides with antiglycation activity. Moreover, the changes in structures and

* Corresponding authors. Tel.: +86 551 2919378; fax: +86 551 2901516.
*E-mail addresses:* xueqiang.zha@upr.edu (X.-Q. Zha), jianpingluo@hfut.edu.cn (J.-P. Luo).

http://dx.doi.org/10.1016/j.carbpol.2014.02.029
0144-8617/

bioactivities were further studied after the polysaccharide structure was modified using chlorosulfonic acid-pyridine (CSA-Pyr) method.

## 2. Materials and methods

### 2.1. Materials and chemicals

*D. huoshanense* C.Z. Tang et S.J. Cheng was collected in Huoshan county, Anhui province of China. The protocorm-like bodies (PLBs) were propagated on Murashige and Skoog medium under 16:8 h light–dark cycle at 25 ± 2 °C (Zha & Luo, 2008). DEAE-cellulose was purchased from Sigma Chemical Co. (MO, USA). Dextran standards were purchased from Fluka Co. (Gallen, Switzerland). Chlorosulfonic acid (CSA), pyridine (Pyr) and formamide were purchased from Guoyao Institute of Chemical Engineering (Shanghai, China). Bovine serum albumin (BSA) was purchased from Sigma Chemical Co. (MO, USA). Nitro blue tetrazolium (NBT) and sodium barbital were obtained from Sinopharm Chemical Reagent Co., Ltd (Shanghai, China). Girard's Reagent T and Aminoguanidine Hydrochloride were purchased from Adamas Reagent Co., Ltd (Shanghai, China). All other reagents were analytical grade.

### 2.2. Extraction and purification of polysaccharides

Fresh PLBs of *D. huoshanense* (1000 g) were homogenized and extracted with distilled water (1/4, w/v) in a water bath (50–60 °C) for three times. The combined extracts were concentrated to 300 mL and mixed with four volume of 99.99% ethanol to precipitate polysaccharides. The precipitates were re-dissolved in distilled water and Sevag method was employed to remove proteins (Staub, 1965). After centrifugation at a speed of 12,000 rpm, the crude polysaccharide solution was fractionated on DEAE-Cellulose column (1.6 × 60 cm) using double distilled water as the mobile phase. The eluent was dialyzed against tap water for 96 h and double distilled water for another 48 h using a bag filter with molecular weight cutoff from 8000 Da to 14,000 Da. The nondialysate was lyophilized to give a purified polysaccharide, named DHPD2.

### 2.3. Preparation of the sulfated polysaccharides

According to the reference (Wang et al., 2010), the DHPD2 powder (100 mg) was dissolved in 5 mL formamide and modified by CSA-Pyr method. The reaction was carried out under the following conditions: 1:2 ratio of CSA to Pyr and 60 °C reaction temperature. After the reaction proceeded for 30 and 60 min, the mixture was cooled to room temperature and the pH was adjusted to 7 with 1 mol/L sodium hydroxide solution. Then the mixture was dialyzed against distilled water for 96 h using a bag filter with molecular weight cutoff from 8000 Da to 14,000 Da. The nondialysate was lyophilized to give the sulfated polysaccharides, named SDHPD21 (sulfated for 30 min) and SDHPD22 (sulfated for 60 min). The degree of sulfate substitution (DS) in sulfated polysaccharides was determined by barium chloride-gelatin method (Dodgson & Price, 1962). The DS was calculated according to the following equation: $DS = [(1.62 \times S\%)/(32 - 1.02 \times S\%)]$. The carbohydrate content was measured by phenol–sulfuric acid method, using D-glucose as a standard (Dubois, Gilles, Hamilton, Rebers, & Smith, 1956).

### 2.4. Homogeneity, molecular weight, monosaccharide composition and glycosyl linkages

The homogeneity and molecular weight of polysaccharides were analyzed by high-performance liquid chromatography (HPLC) according to our previous reports (Zha et al., 2012). The monosaccharide composition of DHPD2 was measured by gas chromatography (GC) with detection condition described in the reference (Zha et al., 2012). The glycosyl linkages were analyzed by methylation method (Pan et al., 2012).

### 2.5. Fourier transformation infrared (FT-IR) spectroscopy and ultraviolet (UV) spectroscopy analysis

The FT-IR spectra of polysaccharides were recorded on a Nicolet Nexus 470 spectrometer between 400 and 4000 $cm^{-1}$. The samples were analyzed as KBr pellets. For UV spectrum, the aqueous solution of polysaccharide was scanned with the wavelength from 190 to 400 nm on a UV–vis spectrophotometer.

### 2.6. Nuclear magnetic resonance (NMR) analysis

DHPD2 and DHPD2-derivatives (60 mg) were deuterium exchanged several times by lyophilizing from $D_2O$ and then examined as solutions in 99.99% $D_2O$ containing a trace of acetone as internal standard. NMR spectra ($^1H$ NMR, $^{13}C$ NMR, HSQC and HMBC) were recorded at 50 °C on a Bruker Avance AV400. Data processing was performed using standard Bruker XWIN-NMR software.

### 2.7. Inhibitory effects of polysaccharides on nonenzymatic glycation of proteins

#### 2.7.1. In vitro glycation of BSA

The BSA/glucose model was employed to evaluate the ability of polysaccharide antiglycation (Wu, Hsieh, Wang, & Chen, 2009). The total 10 mL of reaction mixture contained 20 M BSA, 500 mM glucose and 0.1 or 1.0 mg/mL test samples (DHPD2, SDHPD21, SDHPD22 and aminoguanidine). The negative control only contained BSA and glucose under the same conditions. Aminoguanidine was used as the positive control. All reagents were dissolved in 200 mM barbitone sodium-hydrochloric acid buffer (pH 7.4) and filtrated through 0.22 μm membrane to remove microorganisms. All the mixtures were placed in the dark at 37 ± 0.5 °C. The resulting glycated solution of 1.5 mL was taken out from the whole mixture every 7 days and stored at −20 °C until analysis.

#### 2.7.2. Analysis of Amadori products

The Amadori products were measured by the method of nitro blue tetrazolium (NBT) reductive assay (L.S. Zhang, Wang, & Dong, 2011). The glycated solution of 0.5 mL were mixed with 2.0 mL of 0.3 mM NBT reagent in sodium carbonate buffer (100 mM, pH 10.35), incubated at room temperature for 15 min, and the absorbance was measured at 530 nm.

#### 2.7.3. Analysis of dicarbonyl compounds

Dicarbonyl compound was determined spectrophotometrically by Girard-T assay (L.S. Zhang et al., 2011). The glycated solution of 0.4 mL were mixed with 0.2 mL Girard-T stock solution (500 mM) and 3.4 mL sodium formate (500 mM, pH 2.9), and then incubated at room temperature for 60 min. The absorbance was tested at 294 nm using an UV–vis spectrophotometer.

#### 2.7.4. Analysis of AGEs

The glycated solution of 0.1 mL was diluted to 3 mL with sodium barbital buffer (200 mM, pH 7.4). The fluorescence of AGEs was determined at 370 nm of excitation wavelength and 440 nm of emission wavelength using a sanko 930A spectrofluorometer (L.S. Zhang et al., 2011).

### 2.8. Statistical analysis

All experiments were conducted independently in triplicates and the data were expressed as mean ± standard deviations. All data were analyzed statistically using one-way analysis of variance (ANOVA). Difference was considered to be statistically significant at $p < 0.05$.

## 3. Results and discussion

### 3.1. Purification and physicochemical properties of DHPD2

After purification on DEAE-cellulose anion-exchange chromatography and dialyzation in a bag filter with molecular weight cutoff from 8000 Da to 14,000 Da, one homogeneous and purified polysaccharide was fractionated from PLBs of *D. huoshanense*. According to the calibration curve between the retention time and the logarithms of standard molecular weights, the molecular weight of DHPD2 was estimated to be about $8.09 \times 10^6$ Da. The total carbohydrate content of DHPD2 was estimated to be 92.89% by the phenol–sulfuric acid method. In UV spectrum of DHPD2, absorption at 280 nm and 260 nm was not observed, confirming the absence of proteins and nucleic acids.

As shown in Fig. 1A, the monosaccharide standards of rhamnose, arabinose, xylose, mannose, galactose and glucose were well separated on a GC equipped with HP-5 capillary column, corresponding to the retention times of 14.937, 15.126, 15.427, 19.143, 19.330 and 19.483 min, respectively. According to the GC chromatogram of TFA hydrolyzate of DHPD2, we found that this polysaccharide was mainly composed of galactose, glucose and arabinose in a molar ratio of 0.896:0.723:0.2, along with a trace of mannose, xylose and rhamnose (Fig. 1B). In FT-IR spectrum (Fig. 1C), DHPD2 had a broad stretching intense characteristic peak at around 3398 $cm^{-1}$ for —OH and a weak stretching vibration peak at around 2932 $cm^{-1}$ for C-H. The intense peaks at around 1639 $cm^{-1}$ and 1416 $cm^{-1}$ were referred to C=O asymmetric stretching vibration and symmetric stretching vibration in carbonyl groups. The peak around 1081 $cm^{-1}$ was referred to O-H variable angle vibration of C—O—H. In addition, small characteristic absorptions around 870 and 800 $cm^{-1}$ indicated that DHPD2 contained α- and β-configuration of sugar residues (Chen, Xie, Nie, Li, & Wang, 2008).

### 3.2. Structural characterization of DHPD2

To obtain the linkage information of different sugar residues, the fully methylated DHPD2 was hydrolyzed with TFA, converted to aditol acetates and analyzed by GC–MS. As shown in Table 1, seven types of aditol acetates were observed in the methylated hydrolyzates. Among these products, 2,3-$Me_2$-Ara*p*, 2,3,6-$Me_3$-Glc*p*, 2,3,4-$Me_3$-Glc*p*, 2,3,4-$Me_3$-Gal*p*, 2,4-$Me_2$-Gal*p* and 2,3,6-$Me_3$-Man*p* were the main constituents with a molar ratio of 1.90:3.88:2.97:8.5:0.76:0.71. The product of 2,3,4-$Me_3$-Xyl*p* was observed in a trace. The other component of rhamnose was not detected due to its tiny amount. Therefore, the linkage of glucose was deduced to be (1→4)-linked and (1→6)-linked, the linkage of galactose was (1→6)-linked and (1→3,6)-linked, and the linkage of arabinose was (1→5)-linked. The other glycosyl of xylose and mannose were considered to be the terminal residues. It is suggested that the backbone of DHPD2 might include 1,6-linked galactose, 1,4-linked glucose, 1,6-linked glucose and 1,5-linked arabinose. Moreover, it is easy to find a good correlation between the terminal residues and branched residues, indicating 1-linked xylose and 1-linked mannose were directly or indirectly attached to (1→3,6)-linked galactose. According to these data, we can conclude that DHPD2 is a long-chained hemicellulose with few branches.

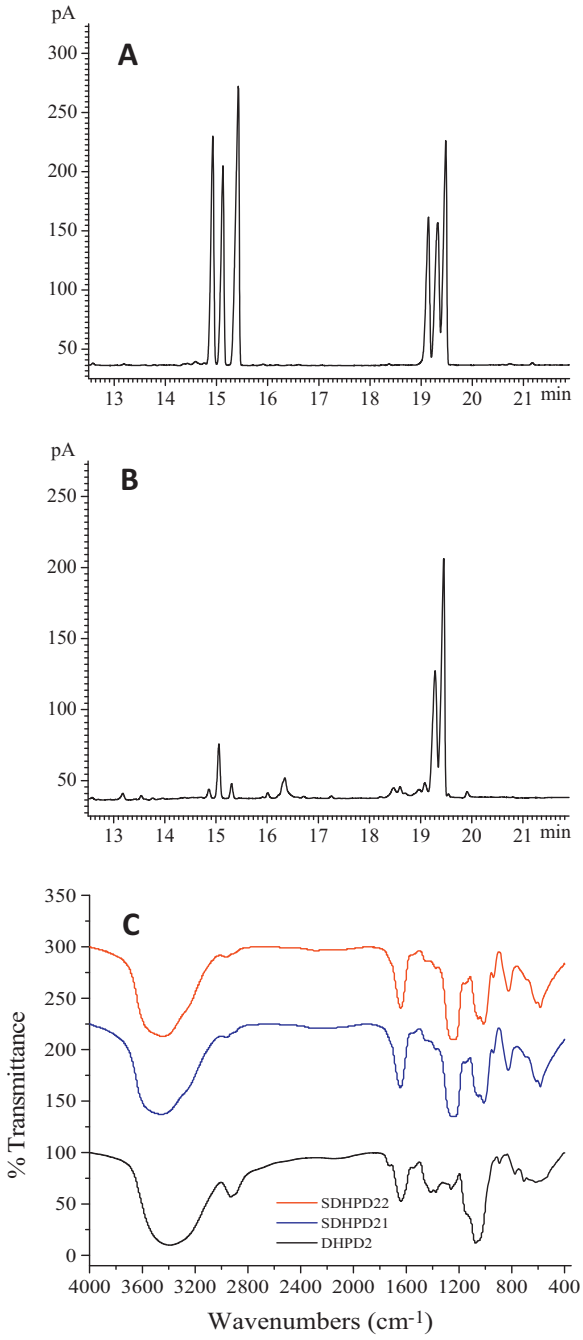


**Fig. 1.** Physicochemical properties of DHPD2. (A) GC chromatography of monosaccharide standards; (B) GC chromatogram of monosaccharides in DHPD2; (C) FT-IR spectrum.

The complete structural features of DHPD2 were characterized from the analysis of NMR spectroscopy. All $^1H$ and $^{13}C$ NMR signals were assigned to the sugar residues using two-dimensional NMR techniques and reference data (Fedonenko, Konnova, & Zatonsky, 2004; Katzenellenbogen, Zatonsky, & Kocharova, 2001; Liu, Sun, & Yu, 2012; Molinaro & Evidente, 2003; Sun, Cui, & Tang, 2010). As shown in Fig. 2A, the chemical shifts of C1 protons were higher or lower than 5.0 ppm, indicating the existence of both α- and β-configuration in DHPD2. This result further confirmed the analysis of FT-IR spectrum. In the anomeric region, the signals at δ 5.17, 5.14, 4.92, 4.91, 4.58, 4.56, 4.48 and 4.42 were assigned to the C1 proton chemical shift of (1→5)-linked α-L-Ara*f*, 1-linked α-D-Xly*p*, (1→6)-linked α-D-Glc*p*, 1-linked

**Table 1**
Methylation analysis data for the polysaccharide of DHPD2.

| Methylated sugar | Characteristic fragments (m/z) | Linkage types | Molar ratio |
|---|---|---|---|
| 2,3-$Me_2$-Ara*p* | 43, 57, 71, 87, 101, 113, 117, 129, 161, 173, 189 | (1→5)-linked Ara*f* | 1.90 |
| 2,3,6-$Me_3$-Man*p* | 43, 55, 71, 87, 99, 113, 129, 147, 159, 173, 233 | 1-Man*p* | 0.71 |
| 2,3,6-$Me_3$-Glc*p* | 43, 71, 87, 101, 117, 129, 143, 161, 233 | (1→4)-linked Glc*p* | 3.88 |
| 2,3,4- $Me_3$-Glc*p* | 43, 58, 71, 87, 101, 117, 129, 161, 189 | (1→6)-linked Glc*p* | 2.97 |
| 2,3,4-$Me_3$-Gal*p* | 43, 58, 71, 87, 101, 117, 129, 161, 173, 233 | (1→6)-linked Gal*p* | 8.5 |
| 2,4-$Me_2$-Gal*p* | 43, 58, 72, 89, 101, 117, 127, 159, 173, 233 | (1→3,6)-linked Gal*p* | 0.76 |
| 2,3,4-$Me_3$-Xyl*p* | 43, 60, 69, 86, 97, 103, 115, 128, 157, 170, 199 | 1-Xyl*p* | Trace |

β-D-Man*p*, (1→6)-linked β-D-Glc*p*, (1→4)-linked β-D-Glc*p*, (1→3,6)-linked β-D-Gal*p* and (1→6)-linked β-D-Gal*p*, respectively. The eight sugar residues were labeled A–H in the order of decreasing C1 proton chemical shifts (Table 2).

The HSQC spectrum showed the correlation of carbons with their respective protons. As shown in Fig. 2B, the cross peaks of δ 109.2/5.17, 109.4/5.14, 99.3/4.92, 97.7/4.91, δ 103.4/4.58, 104.3/4.56, 102.7/4.48 and 103.7/4.42 were obviously observed in the low-field regions of HSQC spectrum. Taken together with the results from $^1$H NMR analysis, it is suggested that the $^{13}$C NMR signals at δ 109.2, 109.4, 99.3, 97.7, δ 103.4, 104.3, 102.7 and 103.7 ppm in a molar ratio of nearly 2:1:1:1:2:4:1:8 were assigned to the chemical shifts of anomeric carbon of (1→5)-linked α-L-Ara*f*, 1-linked α-D-Xyl*p*, (1→6)-linked α-D-Glc*p*, 1-linked β-D-Man*p*, (1→6)-linked β-D-Glc*p*, (1→4)-linked β-D-Glc*p*, (1→3,6)-linked β-D-Gal*p* and (1→6)-linked β-D-Gal*p*, respectively (Fig. 2C). Similarly, complete $^1$H and $^{13}$C NMR signal assignments for sugar residues A–H were obtained and presented in Table 2. The sugar residue sequences were determined by $^1$H–$^{13}$C HMBC experiment. As shown in Fig. 2D, the HMBC spectrum showed strong cross-peaks between $^1$H and $^{13}$C peak in different residues and could be assigned as follows: H H-1 (δ 4.42) and H C-6 (δ 70.9), H H-1 (δ 4.42) and E C-6 (δ 69.9), E H-1 (δ 4.58) and G C-6 (δ 69.3), G H-1 (δ 4.48) and A C-5 (δ 68.4), A H-1 (δ 5.17) and F C-4 (δ 78.3), F H-1 (δ 4.56) and F C-4 (δ 78.3), F H-1 (δ 4.56) and A C-5 (δ 68.4), F H-1 (δ 4.56) and E C-6 (δ 69.9), E H-1 (δ 4.58) and C C-6 (δ 68.3) and C H-1 (δ 4.92) and H C-6 (δ 70.9). Therefore, the possible sequences of residues A, C, E, F, G and H in the backbone of DHPD2 was assigned as follows:

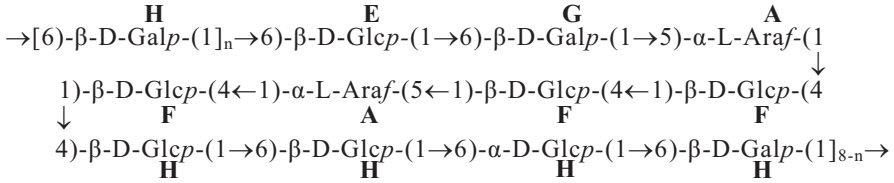


The other cross-peaks between H-1 of residues B (δ 5.14) and C-3of residues G (δ 83.8), and H-1 of residues D (δ 4.91) and C-3 of residues G (δ 83.8) supported the residue sequence of B, D and G as follows:

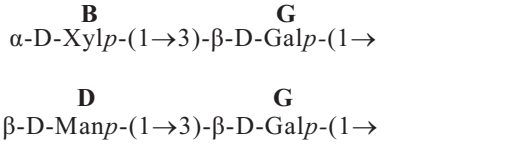


Based on all these chemical and NMR spectra findings, the possible structure of the repeating unit of DHPD2 was presented in Fig. 2E.

### 3.3. Preparation and physicochemical properties of DHPD2 sulfated derivatives

The CSA-Pyr method was performed to modify the chemical structure of DHPD2. After the sulfated esterification was carried out for 30 min and 60 min, two sulfated derivatives (SDHPD21 and SDHPD22) were obtained. The molecular weight was calculated as $1.10 \times 10^7$ Da for SDHPD21 and $1.01 \times 10^7$ Da for SDHPD22.

**Table 2**
$^{13}$C and $^1$H NMR chemical shifts (ppm) for the polysaccharide of DHPD2.

| | Sugar residues | | 1 | 2 | 3 | 4 | 5 | 6 |
|---|---|---|---|---|---|---|---|---|
| A | →5-α-L-Ara*f*(1→ | H | 5.17 | 4.13 | 3.85 | 4.13 | 3.86 | |
| | | C | 109.2 | 83.7 | 74.8 | 83.9 | 68.4 | |
| B | α-D-Xyl*p*(1→ | H | 5.14 | 3.45 | 3.68 | 3.58 | 3.52 | |
| | | C | 109.4 | 73.4 | 73.1 | 71.3 | 62.3 | |
| C | →6-α-D-Glc*p*(1→ | H | 4.92 | 3.44 | 3.81 | 3.60 | 3.83 | 3.92 |
| | | C | 99.3 | 72.5 | 73.3 | 69.5 | 72.5 | 68.3 |
| D | β-D-Man*p*(1→ | H | 4.91 | 3.94 | 3.61 | 3.67 | 3.42 | 3.84 |
| | | C | 97.7 | 79.6 | 73.0 | 68.1 | 77.7 | 61.3 |
| E | →6-β-D-Glc*p*(1→ | H | 4.58 | 3.48 | 3.62 | 3.42 | 3.80 | 4.05 |
| | | C | 103.4 | 73.8 | 75.5 | 70.4 | 75.1 | 69.9 |
| F | →4-β-D-Glc*p*(1→ | H | 4.56 | 3.58 | 3.66 | 3.61 | 3.52 | 3.68 |
| | | C | 104.3 | 73.2 | 75.1 | 78.3 | 74.9 | 61.1 |
| G | →3,6-β-D-Gal*p*(1→ | H | 4.48 | 3.60 | 4.12 | 4.33 | 3.61 | 3.77 |
| | | C | 102.7 | 72.7 | 83.8 | 69.8 | 76.5 | 69.3 |
| H | →6-β-D-Gal*p*(1→ | H | 4.42 | 3.45 | 3.67 | 3.94 | 3.81 | 3.88 |
| | | C | 103.7 | 72.6 | 72.7 | 68.5 | 74.9 | 70.9 |

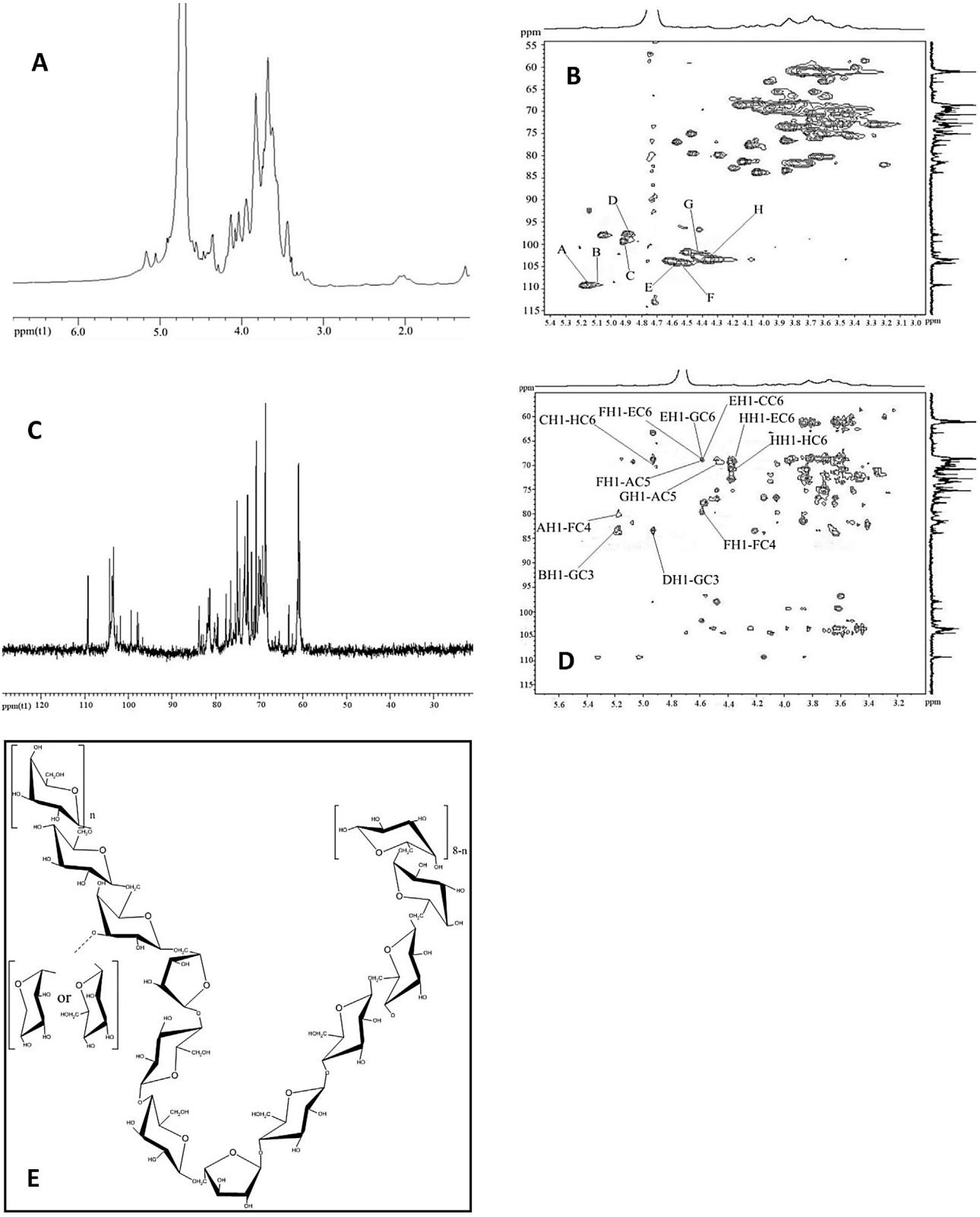


**Fig. 2.** NMR spectra and possible repeat unit of DHPD2. (A) $^{1}$H NMR; (B) HSQC; (C) $^{13}$C NMR; (D) HMBC; (E) possible repeat unit.

The DS was determined as 0.475 for SDHPD21 and 0.940 for SDHPD22. Meanwhile the carbohydrate contents were determined as 56.35% and 37.7% for SDHPD21 and SDHPD22, respectively. By comprehensive analysis of molecular weight, DS and carbohydrate content information, it is revealed that sulfated esterification caused DHPD2 degradation. Compared with DHPD2, two new characteristic absorption bands were observed in the FT-IR spectra of sulfated derivatives (Fig. 3). The intense absorption peak at around 1250 $cm^{-1}$ was attributed to an asymmetrical S=O stretching vibration of C—O—$SO_3$ group (Saha & Navid, 2012; Yang, Du, & Huang,

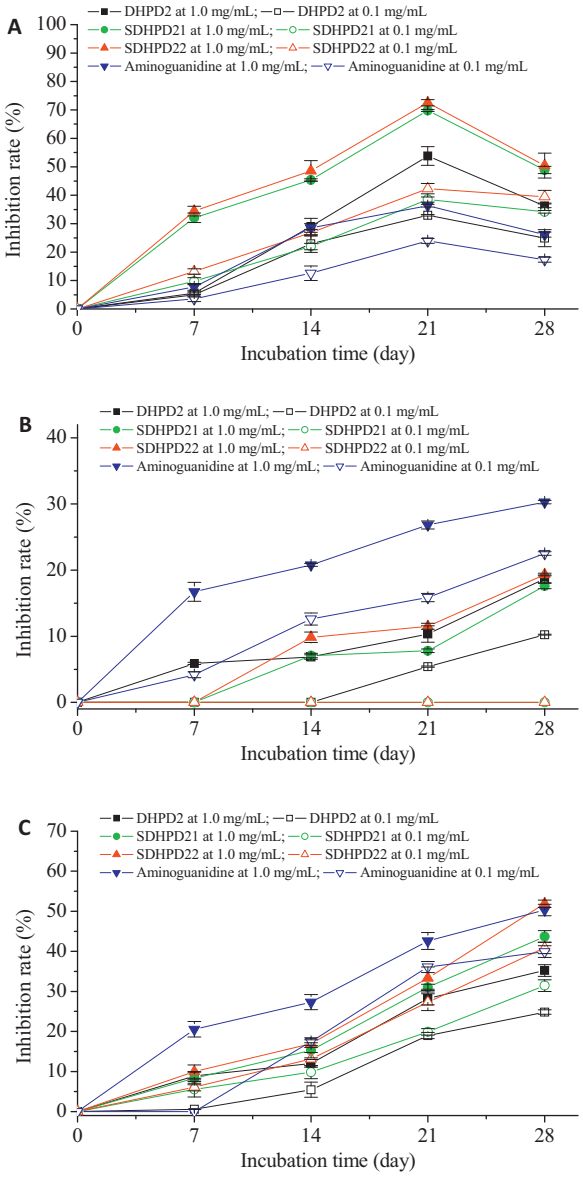


**Fig. 3.** Inhibitory effects of DHPD1, SDHPD21, SDHPD22 and aminoguanidine on the process of protein non-enzymatic glycation. (A) Inhibit Amadori product formation; (B) inhibit dicarbonyl compound formation; (C) inhibit AGE formation.

2002). The absorption peak at around 822 $cm^{-1}$ was caused by symmetrical stretching vibration of C—O—S associated with a C—O—$SO_3$ group (Saha & Navid, 2012; Yang et al., 2002). It has been reported that the position of sulphate group in polysaccharide could be deduced by the infrared absorption region around 800–850 $cm^{-1}$ (L. Wang, Huang, & Wei, 2009). The absorption bands near 820 $cm^{-1}$ were assigned to the sulfate group attached to the C-6 and C-2 position of sugar residues. The absence of bands near 845 $cm^{-1}$ suggested the substitution of sulfate group did not occurred to the C-4 position. Accordingly, we can infer that the hydroxyl groups attached to C-6 and C-2 of galactose residues were easily substituted by sulfate groups.

### 3.4. Inhibitory effects of polysaccharides on protein glycation

It is accepted that the non-enzymatic glycation of proteins includes three reaction phases, namely early phase, intermediate phase and late phase. To inhibit any process can alleviate the formation of AGEs. In the early phase, the reducing sugar reacts with the free amino groups of proteins to form schiff base, and then rearrange to form Amadori products (Lapolla, Traldi, & Fedele, 2005). As shown in Fig. 3A, all polysaccharides exhibited strong inhibitory activities on the formation of Amadori products in a dose-dependent manner. These inhibitory activities of all agents at different dosage were enhanced with the culture proceeding from 0 to 21 days and then decreased to different levels. In addition, the inhibitory capability of all agents was revealed to be in the order of SDHPD22 > SDHPD21 > DHPD2 > aminoguanidine. The maximal inhibitory rate (72.54%) on the formation of Amadori products was observed in the group treated with 1.0 mg/mL SDHPD22 at the culture time of 21st day, which was 1.31-fold and 1.95-fold than that of DHPD2 and aminoguanidine, respectively. In the intermediate phase, the Amadori products are converted to dicarbonyl compounds such as methylglyoxal, glyoxal and deoxyglucosones through oxidation and dehydration reactions (Wu et al., 2009). These dicarbonyl compounds were reported to be more reactive than their donors and easily continue to react with amino groups to produce AGEs (L.S. Zhang et al., 2011), indicating the inhibitory actions on dicarbonyl compounds formation might play a critical role in determining the inhibitory capabilities of therapeutical agents on AGE formation. As shown in Fig. 3B, higher dosage (1.0 mg/mL) of each agent was beneficial to inhibit the formation of dicarbonyl compounds. Meanwhile, the inhibitory ability was not observed for the two sulfated DHPD2 derivatives at 0.1 mg/mL. In the last phase, the AGEs were irreversibly produced. Fig. 4C shows the time course of AGEs formation in the presence of DHPD2, sulfated DHPD2 derivatives and aminoguanidine. For each agent at different dosage, the inhibitory rate increased gradually from 0 day to 28 days of incubation. With regard to inhibitory ability of different agents at the same dosage, it was decreased in the order of aminoguanidine > SDHPD22 > SDHPD21 > DHPD2. After 28 days of incubation, SDHPD22 at 1.0 mg/mL showed the highest inhibitory ability of 51.9%, which increased by 18% and 47% than that of SDHPD21 and DHPD2 at the same dosage. It has been reported that free radicals play an important role in the process of non-enzymatic glycation of proteins. In recent years, some natural products have been reported to exhibit antiglycation activities, which were correlated to their antioxidant properties (Dai & Mumper, 2010; Ramkissoon, Mahomoodally, Ahmed, & Subratty, 2013; Xi et al., 2010). In our previous works, polysaccharides extracted from *D. huoshanense* have been confirmed to possess strong potential for preventing lipid peroxidation and scavenging free radicals (superoxide anion, hydroxyl free radical and hydrogen peroxide) in vitro (Hao, Zha, Bao, & Luo, 2009). Therefore, we speculated that the inhibitory actions of *D. huoshanense* polysaccharides and their sulfated derivatives on protein non-enzymatic glycation were attributed to their antioxidant properties.

### 3.5. Relationships between sulfated position and antiglycation activities

Sulfated modification has been reported to be an effective method to improve polysaccharide bioactivities, such as antitumor, anti-oxidant and anti-coagulation (Cardozo et al., 2013; Wang et al., 2010). In the present study, we found that the inhibitory activities of *D. huoshanense* polysaccharide on protein non-enzymatic glycation were also strongly enhanced by sulfated modification (Fig. 3). It is accepted that the biological activity of sulfated polysaccharides were dependent on their structural features including the degree of substitution, the molecular weight (Mw) and the position of sulfation occurrence. With respect to *D. huoshanense* polysaccharide, the higher DS of DHPD2 sulfated derivatives, the stronger activity was observed to inhibit protein non-enzymatic glycation. The position of sulfation occurred to polysaccharides can be determined by NMR technologies (Y.L. Zhang, Lu, Fu, Wang, &

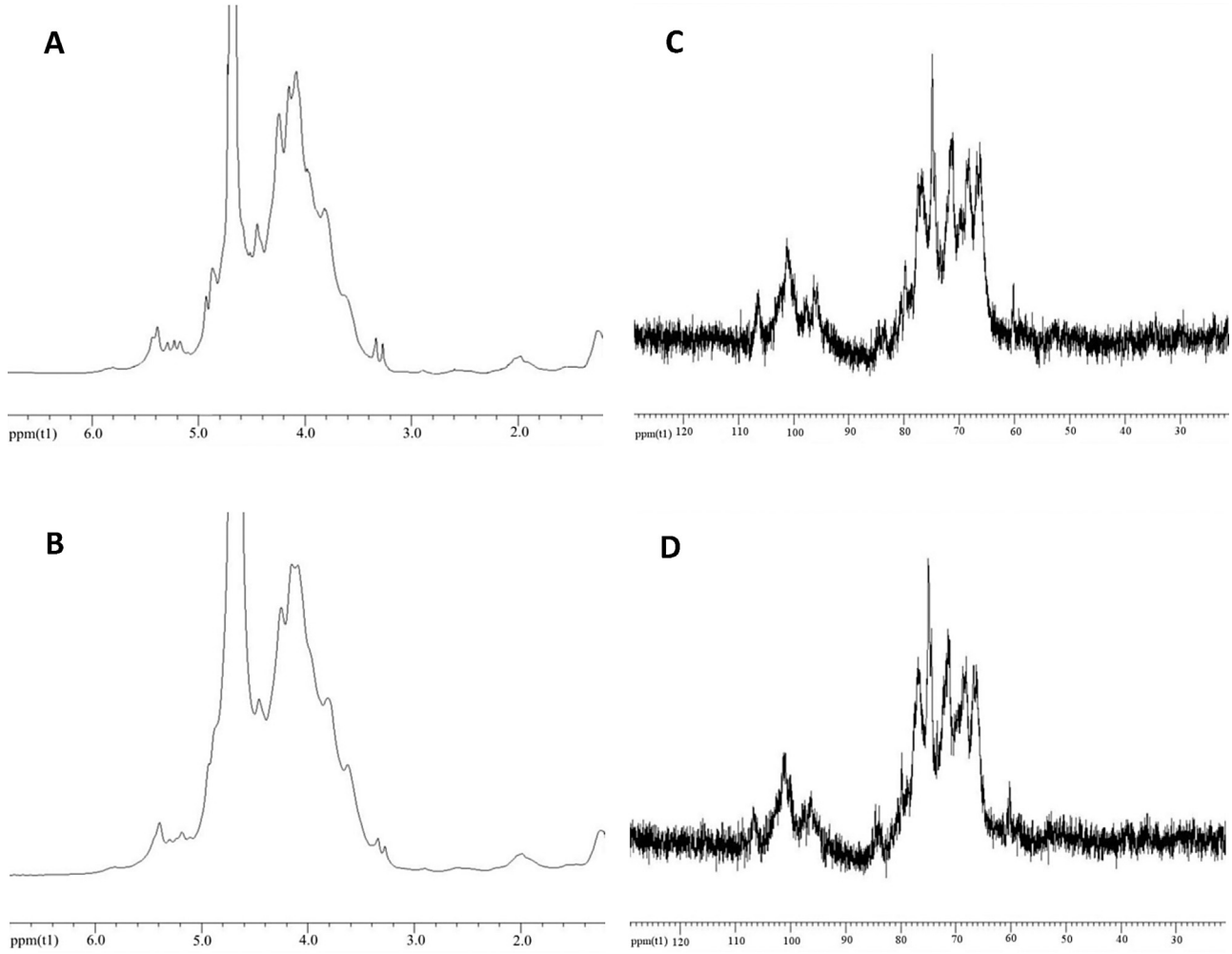


**Fig. 4.** NMR spectra of DHPD2 sulfated derivatives. (A) $^{1}$H NMR of SDHPD21; (B) $^{1}$H NMR of SDHPD22; (C) $^{13}$C NMR of SDHPD21; (D) $^{13}$C NMR of SDHPD22.

Zhang, 2011; Liu et al., 2009; Wang et al., 2010). In comparison with DHPD2, different resonances appeared between 3.4 and 4.8 ppm (protons of sulfated positions) in the $^{1}$H NMR spectra of DHPD2 sulfated derivatives (Fig. 4A and B), suggesting the sulfate groups were attached to DHPD2 after modification. Fig. 4C and D shows the carbon chemical shifts of SDHPD21 and SDHPD22, respectively. Compared to the $^{13}$C NMR spectrum of DHPD2 (Fig. 2C), the sulfated DHPD2 derivatives exhibited more complicated signals because of the presence and absence of sulfate groups in polysaccharides, which might be due to the result of spectra with a high degree of overlapping. It has been reported that the carbon directly attached to an electron-withdrawing sulfate group would shift to a lower field position, while the carbon indirectly attached to sulfate group would shift to higher field position (Wang et al., 2010). After sulfated modification, the carbon signals of chemical shifts at near 60 ppm were significantly weakened while the signals at near 67 ppm in the spectrum of DHPD2 were strongly enhanced (Fig. 4C and D), indicating that some OH groups on the C6 of 1-linked β-D-Man*p* and 1,4-linked β-D-Glc*p* were substituted by sulfated groups. Similarly, the signals from 72 to 74 ppm were observed to be weakened as well as those near 83 ppm, and the chemical shifts from 75 to 76 ppm were enhanced, supporting the fact that sulfation has occurred to OH group on the C2 of sugar residues. The other evidences revealed that the anomeric carbon signals could be split into two peaks when the OH groups on C2 were replaced by sulfate groups (Wei, Wei, Cheng, & Zhang, 2012). Meanwhile, this splitting of C1 signals correlated well with the extent of substitution at the C2 atom (Liu et al., 2009). In the present study, the anomeric carbon signals from about 102 to 104 ppm and 97 to 100 ppm were weakened while the signals from about 106 to 108 ppm and 101 to 102 ppm were drastically strengthened in the low-field region, further indicating the OH groups on the C2 were actually substituted by sulfate groups. Moreover, combined with the results of activity investigation, it is concluded that sulfation occurred to C-2 and C-6, were beneficial to improve the antiglycation activity of DHPD2.

## 4. Conclusions

An active polysaccharide DHPD2 with molecular weight of $8.09 \times 10^{6}$ Da was extracted from PLBs of *D. huoshanense*, which was free of proteins. Chemical structure analysis revealed that DHPD2 was a long-chained hemicellulose with few branches. The CSA-Pyr method was performed to modify the structure of DHPD2, giving two sulfated derivatives named SDHPD21 and SDHPD22. The DS of SDHPD21 and SDHPD22 were determined as 0.475 and 0.940, respectively. Structural analysis revealed that sulfation occurred to C-2 and C-6 of glycosyl residues, was beneficial to enhance the antiglycation activity of DHPD2.

## Acknowledgements

This research was supported by the National Natural Science Foundation of China (grant nos. 21006019, 31271814 and 20872024), the International Foundation for Science and the

Organization for the Prohibition of Chemical Weapons (grant no. F/4577-1), and the project for Science and Technology Research Plant from Anhui Province of China (grant no. 12010402088).

## References


Cardozo, F. T. G. S., Camelini, C. M., Cordeiro, M. N. S., Mascarello, A., Malagoli, B. G., Larsen, I. V., et al. (2013). Characterization and cytotoxic activity of sulfated derivatives of polysaccharides from *Agaricus brasiliensis*. *International Journal of Biological Macromolecules*, *57*, 265–272.

Chen, Y., Xie, M. Y., Nie, S. P., Li, C., & Wang, Y. X. (2008). Purification, composition analysis and antioxidant activity of a polysaccharide from the fruiting bodies of *Ganoderma atrum*. *Food Chemistry*, *107*, 231–241.

Dai, J., & Mumper, R. J. (2010). Plant phenolics: Extraction, analysis and their antioxidant and anticancer properties. *Molecules*, *15*, 7313–7352.

Dodgson, K. S., & Price, R. G. (1962). A note on the determination of the ester sulphate content of sulphated polysaccharides. *Biochemical Pharmacology*, *84*, 106–110.

Dubois, M., Gilles, K. A., Hamilton, J. J., Rebers, P. A., & Smith, F. (1956). Colormetric method for the determination of sugars and related substances. *Analytical Chemistry*, *28*, 350–356.

Fedonenko, Y. P., Konnova, O. N., & Zatonsky, G. V. (2004). Structure of the O-polysaccharide of the lipopolysaccharide of *Azospirillum irakense* KBC1. *Carbohydrate Research*, *339*, 1813–1816.

Hao, J., Zha, X. Q., Bao, S. H., & Luo, J. P. (2009). In vitro antioxidant activities of polysaccharides with different molecular mass from seedlings of *Dendrobium huoshanense*. *Chinese Food Science*, *28*, 90–92.

Hsieh, S. Y., Chien, C., Liao, K. S., Liao, S. F., Hung, W. T., & Yang, W. B. (2008). Structure and bioactivity of the polysaccharides in medical plant *Dendrobium huoshanense*. *Bioorganic & Medicinal Chemistry*, *16*, 6056–6068.

Huang, S. W., & Zhang, J. (2000). Precious *Dendrobium huoshanense*. *Anhui Medical and Pharmaceutical Journal*, *4*, 42–43 (in Chinese).

Jagtap, A. G., & Patil, P. B. (2010). Antihyperglycemic activity and inhibition of advanced glycation end product formation by *Cuminum cyminumin* streptozotocin induced diabetic rats. *Food and Chemical Toxicology*, *48*, 2030–2036.

Katzenellenbogen, E., Zatonsky, G. V., & Kocharova, N. A. (2001). Structure of the O-specific polysaccharide of *hafnia alve*i PCM 1196. *Carbohydrate Research*, *330*, 523–528.

Kumar, P. A., Reddy, P. Y., Srinivas, P. N. B. S., & Reddy, G. B. (2009). Delay of diabetic cataract in rats by the antiglycating potential of cumin through modulation of α-crystallin chaperone activity. *Journal of Nutritional Biochemistry*, *20*, 553–562.

Lapolla, A., Traldi, P., & Fedele, D. (2005). Importance of measuring products of non-enzymatic glycation of proteins. *Clinical Biochemistry*, *38*, 103–115.

Li, X. F., Deng, Y. Y., Pan, L. H., Huang, J., & Luo, J. P. (2012). Antioxidant effect of polysaccharide from *Dendrobium huoshanense* on lens tissue of diabetic cataract rats. *Chinese Traditional Patent Medicine*, *34*, 418–421 (in Chinese).

Liu, J. C., Sun, Y. X., & Yu, H. T. (2012). Purification and identification of one glucan from golden oyster mushroom (*Pleurotus citrinopileatus* (Fr.) Singer). *Carbohydrate Polymers*, *87*, 348–352.

Liu, Y. H., Liu, C. H., Tan, H. N., Zhao, T., Cao, J. C., & Wang, F. S. (2009). Sulfation of a polysaccharide obtained from *Phellinus ribisand* potential biological activities of the sulfated derivatives. *Carbohydrate Polymers*, *77*, 370–375.

Liu, Y., & Luo, J. P. (2005). Optimization conditions for liquid culture of protocorm-like bodies of *Dendrobium huoshanenes*. *Chinese Food Science*, *26*, 84–87 (in Chinese).

Luo, J. P., Deng, Y. Y., & Zha, X. Q. (2008). Mechanism of polysaccharides from *Dendrobium huoshanense* on streptozotocin-induced diabetic cataract. *Pharmaceutical Biology*, *46*, 243–249.

Molinaro, A., & Evidente, A. (2003). Structural determination of a novel O-chain polysaccharide of the lipopolysaccharide from the bacterium *Xanthomonas campestris* pv. Pruni. *European Journal of Organic chemistry*, *12*, 2254–2259.

Pan, D., Wang, L., Chen, C., Teng, B., Wang, C., Xu, Z., et al. (2012). Structure characterization of a novel neutral polysaccharide isolated from *Ganoderma lucidum* fruiting bodies. *Food Chemistry*, *135*, 1097–1103.

Ramkissoon, J. S., Mahomoodally, M. F., Ahmed, N., & Subratty, A. H. (2013). Antioxidant and anti-glycation activities correlates with phenolic composition of tropical medicinal herbs. *Asian Pacific Journal of Tropical Medicine*, *6*(7), 561–569.

Saha, S., & Navid, M. H. (2012). Sulfated polysaccharides from *Laminaria angustata*: Structural features and in vitro antiviral activities. *Carbohydrate Polymers*, *87*, 123–130.

Singh, R., Barden, A., Mori, T., & Beilin, L. (2001). Advanced glycation end-products: A review. *Diabetologia*, *2*, 126–129.

Staub, A. M. (1965). Removeal of protein-Sevag method. *Methods in Carbohydrate Chemistry*, *5*, 5–6.

Sun, Y. L., Cui, S. W., & Tang. (2010). Structural features of pectic polysaccharide from *Angelica sinensis* (Oliv.) Diels. *Carbohydrate Polymers*, *80*, 544–550.

Wada, R., Nishizawa, Y., Yagihashi, H., Takeuchi, M., Ishikawa, Y., Yasumura, K., et al. (2002). Inhibition of the development of experimental diabetic neuropathy by suppression of AGE formation with a new antiglycation agent. *International Congress Series*, *1245*, 101–105.

Wang, J., Sun, B. J., Cao, Y. P., & Tian, Y. (2009). Protein glycation inhibitory activity of wheat bran feruloyl oligosaccharides. *Food Chemistry*, *112*, 350–353.

Wang, L., Huang, H. Y., & Wei, Y. Y. (2009). Characterization and anti-tumor activities of sulfated polysaccharide SRBPS2a obtained from defatted rice bran. *International Journal of Biological Macromolecules*, *45*, 427–431.

Wang, X. F., Wang, J. L., Zhang, L., Zhao, B. T., Yao, J., & Wang, Y. P. (2010). Structure-antioxidant relationships of sulfated galactomannan from guar gum. *International Journal of Biological Macromolecules*, *46*, 59–66.

Wang, X., Zhang, L. S., & Dong, L. L. (2012). Inhibitory effect of polysaccharides from pumpkin on advanced glycation end-products formation and aldose reductase activity. *Food Chemistry*, *130*, 821–825.

Wei, D. F., Wei, Y. X., Cheng, W. D., & Zhang, L. F. (2012). Sulfated modification, characterization and antitumor activities of *Radix hedysari* polysaccharide. *International Journal of Biological Macromolecules*, *51*, 471–476.

Wu, J. W., Hsieh, C. L., Wang, H. Y., & Chen, H. Y. (2009). Inhibitory effects of guava (*Psidium guajava* L.) leaf extracts and its active compounds on the glycation process of protein. *Food Chemistry*, *113*, 78–84.

Xi, M., Hai, C., Tang, H., Chen, M., Fang, K., & Liang, X. (2010). Antioxidant and antiglycation properties of total saponins extracted from traditional Chinese medicine used to treat diabetes mellitus. *Phytotherapy*, *22*, 228–237.

Yang, J. H., Du, Y. M., & Huang, R. H. (2002). Chemical modification, characterization and structure-anticoagulant activity relationship of *Chinese lacquer* polysaccharides. *International Journal of Biological Macromolecules*, *31*, 55–62.

Zha, X. Q., & Luo, J. P. (2008). Production stability of active polysaccharides of *Dendrobium huoshanense* using long-term cultures of protocorm-like bodies. *Planta Medica*, *74*, 90–93.

Zha, X. Q., Xiao, J. J., Zhang, H. L., Wang, J. H., Pan, L. H., Yang, X. F., et al. (2012). Polysaccharides in *Laminaria japonica* (LP): Extraction, physicochemical properties and their hypolipidemic activities in diet-induced mouse model of atherosclerosis. *Food Chemistry*, *134*, 244–252.

Zhang, L. S., Wang, X., & Dong, L. L. (2011). Antioxidation and antiglycation of polysaccharides from *Misgurnus anguillicaudatus*. *Food Chemistry*, *124*, 183–187.

Zhang, Y. L., Lu, X. Y., Fu, Z. B., Wang, Z. B., & Zhang, J. B. (2011). Sulphated modification of a polysaccharide obtained from fresh persimmon (*Diospyros kaki* L.) fruit and antioxidant activities of the sulphated derivatives. *Food Chemistry*, *127*, 1084–1090.